Journal Name

ARTICLE

Metal-mediated linear self-assembly of porphyrins

J. A. Wytko,[a] R. Ruppert,[a*] C. Jeandon,[a] and J. Weiss[a*]

Received 00th January 20xx,
Accepted 00th January 20xx

Porphyrin derivatives are highly relevant to biological processes such as light harvesting and charge separation. Their aromatic electronic structure and their accessible HOMO-LUMO gap render porphyrins highly attractive for the development of opto- and electro-active materials. Due to the often difficult covalent synthesis of multiporphyrins, self-assembly using metal complexation as the driving force can lead to well defined objects exhibiting a controlled morphology, which will be required to analyse and understand the electronic properties of porphyrin wires. This article presents two assembly approaches, namely by peripheral coordination or by binding to a metal ion in the porphyrin core, that are efficient and well designed for future developments requiring interactions with a surface.

DOI: 10.1039/x0xx00000x

www.rsc.org/

Introduction and scope

Porphyrins…. naturally!

Porphyrins are a class of tetrapyrrolic macrocycles in which four pyrrole rings are connected *via* methine bridges (Chart 1). Due to their aromatic character and thus accessible HOMO-LUMO gap, porphyrin derivatives are stable and highly coloured. Consequently, porphyrin derivatives have been selected as the pigments of life[1] through billions years of evolution and, thus, play major roles in Nature.

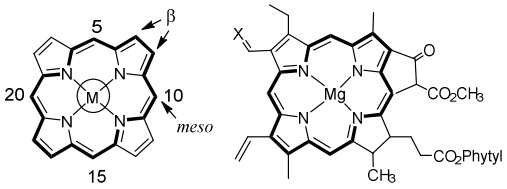

Chart 1. Structure of the porphyrin macrocycle (M≠H_2: metalloporphyrin) and of chlorophyll (*a*: X=CH_2, *b*: X=O). In both structures, the aromatic pathway is indicated in bold.

This tetrapyrrolic core and its derivatives are found in all the photonic collection and conversion processes of plants and photosynthetic bacteria. Chart 1 shows the structures of chlorophylls *a* and *b* together with the parent porphyrin ring and the labelling of its possible substitution pattern. The structure of a bacterial photosynthetic reaction centre (RC) represented in Figure 1 was published in 1985.[2] This structure stimulated a wide range of synthetic research aimed at

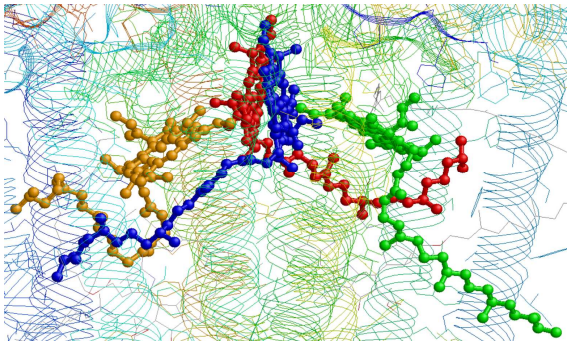

Figure 1. Partial representation of the reactive center (RC) of Rhodopseudomonas Viridis (1PRC).

reproducing the RC's geometric features, especially the distances and angles between the chromophores, to explore electronic interactions in both ground and excited states. At first, this research led to a series of kinked bis-porphyrin scaffolds such as the two historical examples represented in Chart 2 from the groups of Sessler[3] and Sauvage.[4] The scaffolds were meant to reproduce the oblique orientation of the two bacteriochlorophylls (BChl) (in green and orange in

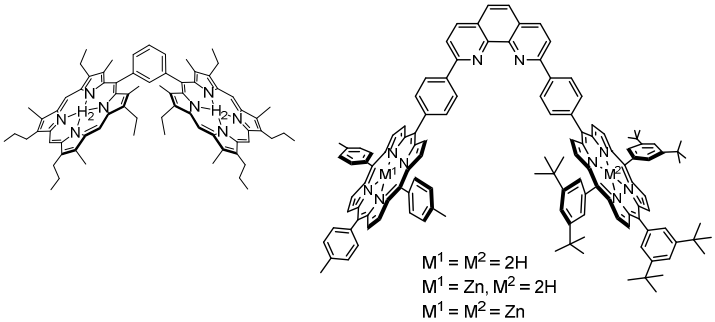

Chart 2. Two oblique bis-porphyrins mimicking particular arrangements of the BChl in the bacterial photosynthetic reaction centre.

[a] Institut de Chimie de Strasbourg, UMR 7177 CNRS-Université de Strasbourg, 4 rue Blaise Pascal, 67000 STRASBOURG, France.

† Footnotes relating to the title and/or authors should appear here.
Electronic Supplementary Information (ESI) available: [details of any supplementary information available should be included here]. See DOI: 10.1039/x0xx00000x

Figure 1) next to the special pair (in blue and red in Figure 1).

Another source of inspiration and challenge in synthetic porphyrin chemistry arose upon publication of the circular structures of the light harvesting (LH) antennae systems LH1 and LH2. These circular arrangements of chromophores are responsible for transporting photonic energy over long distances in plants[5] or in bacteria.[6,7]

In the bacterial LH2 antenna,[8] the BChl850 (absorbing at 850 nm) are closely packed at van der Waals distances, as shown by the red circles in Figure 2a. The general orientation of each chromophore is highlighted by the grey bars. This arrangement allows orbital overlap between neighbouring chromophores and a delocalisation of the photonic energy around the circular arrangement *via* a mixture of Dexter[9] and Förster[10] mechanisms.

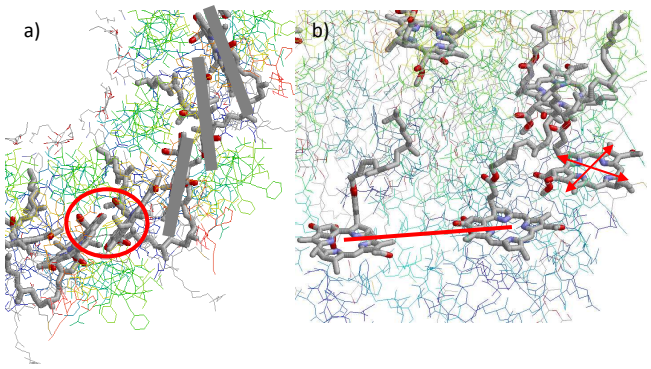

Figure 2. Enlargement of the spatial arrangement of a) the BChl850 chromophores; b) the BChl800 chromophores in the LH2 unit of *Rhodopseudomonas acidophila. Images generated from the PDB file 1nkz.*

The spatial arrangement of the BChl800 shows a larger spacing of 22.2 Å between the chromophores (red line, Figure 2b), suggesting communication by a Förster resonance transfer, which is favoured by the appropriate orientation of the transition dipole moments of the chromophores (red criss-crossed arrows).[11] The same mechanism is expected for the energy transfer over 18 Å from the BChl800 to the BChl 850 in the energy cascade that funnels photonic energy to the RC via the LH1.[12]

From photosynthesis to nanomaterials

The implication of porphyrinoid derivatives in a wide range of natural processes has been an everlasting source of ideas for bioinspired structures and multiporphyrin scaffolding. Over the last few decades, the field of porphyrin self-assembly has significantly evolved in both its goals and the means to reach them. Early work on multiporphyrin scaffolds aimed at better understanding the factors governing energy and electron transfer in Nature through the use of geometrically well-defined molecular dyads[4] and triads.[13] Interest in multiporphyrins has gradually shifted towards self-assembled nano-objects for photoactive supramolecular devices. More recently, the emergence of nanosciences and molecular electronics,[14] combined with the pronounced pi-conjugated character of porphyrin derivatives, stimulated a strong interest in porphyrin nanomaterials, and particularly in nanowires or one-dimensional assemblies.[15]

Spatial arrangement and ground state interactions

Porphyrin-based chromophores usually display two sets of absorption bands, the Soret band, corresponding to the S_0-S_2 transition at 400-450 nm, and Q bands at *ca*. 500 nm and higher and that correspond to the S_0-S_1 transition and a symmetry-dependent number of vibrational states. The lowest energy Q band corresponds to the HOMO-LUMO gap and any variation of the absorption pattern for a given porphyrin is representative of changes in this gap. In the absence of a central metal or when the latter is not electroactive, the first reduction and oxidation processes occur on the macrocycle. Therefore, the HOMO-LUMO can be measured by cyclic voltammetry.

In linear self-assembly, the degree of electronic interaction between chromophores can thus be evaluated in the ground state by UV-visible spectrophotometry. In the case of multi-

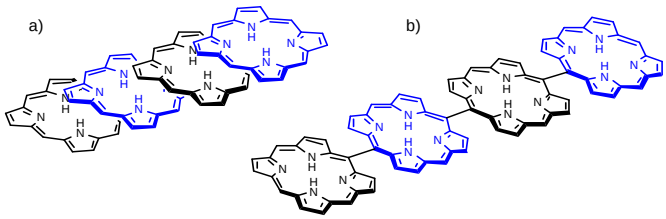

Chart 3. J-aggregate (left) and covalent, *meso-meso*- linked porphyrins.

porphyrin assemblies, the term J-aggregate (Chart 3a) is used to describe an overlapping organisation leading to red-shifted absorption bands. The arrangement of the BChl850 in Figure 2a is a representative example of J-aggregates. As shown in Chart 3b, the *meso-meso* linking of porphyrins represents the covalent version of strongly interacting subunits, given that all chromophores are maintained in the same plane.

In the case of covalent linear assemblies, electrochemistry is a useful tool to evaluate ground state interactions. The two early examples represented in Scheme 1 show how co-planarity of the two porphyrin planes influences the extension of electronic delocalisation and reduces the HOMO-LUMO gap in the coupled chromophores. Whereas the butadiyne-linked dimer (Scheme 1a), reported by Lindsey,[16] displays absorption properties that are very similar to the isolated single porphyrin with a Soret at 422 nm and Q bands at 550 and 588 nm, the ethyne-linked dimer described by Therien[17] shows strong excitonic coupling in both the ground and excited states. The interactions are particularly noticeable due to a distorted, split Soret band leading to two absorptions at 420 and 480 nm and a red-shifted Q band at 640 nm instead of 540 nm in the monomer. In the butadiyne dimer, the presence of phenyl spzcers at the *meso* positions of the porphyrins prevents conjugation of both macrocycles. With an ethyne spacer, the existence of a cumulenic form (Scheme 1b) in the excited state

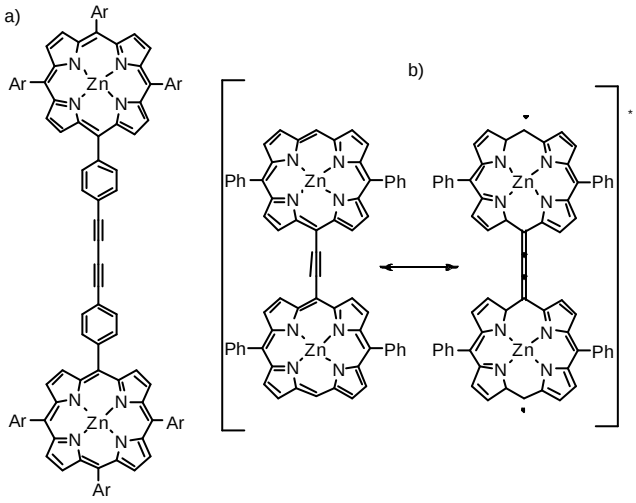

Scheme 1. a) A butadiyne linked porphyrin dimer; b) An ethyne linked dimer and its resonant cumulenic form in the excited state.

explains strong interactions in the excited emissive state. However, in the ground state, the excitonic interactions are strong due to the orientation of the transition dipole moments, although delocalisation is minimal or inexistent.

One of the longest extensions of conjugation affecting both the ground and the excited states is reached when porphyrin macrocycles are fused. The synthesis of directly linked porphyrins, such as the tetramer[18] of Chart 4a and the doubly fused dimer[19] reported three years apart by Osuka and co-workers, has greatly helped to decipher how coplanarity influences the electronic states of the chromophores. For long oligomers, the HOMO-LUMO gap decreased such that absorption in the infrared was observed.[20]

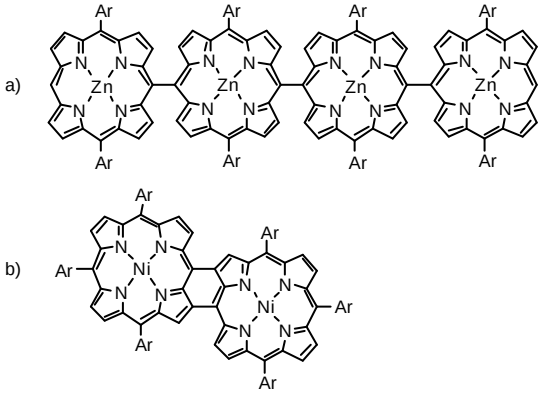

Chart 4. a) A directly linked porphyrin tetramer; b) A doubly linked (or fused) porphyrin dimer.

These historical examples have stimulated a great deal of synthetic effort aimed at the sophistication of the electronic and optoelectronic properties of molecular devices combining multiple porphyrins.[21-23] In general, the preparation of covalent assemblies is not compatible with large scale production of the compounds. In some cases, the iterative aspects of a synthetic pathway hold promise for facilitated access to large species; however, often the parallel with a polymerisation-based approach leads to a partial loss of control of the oligomers' morphology.[24] New methods were thus necessary to obtain long, yet well organised porphyrin oligomers in order to develop concepts that would lead in future applications. Self-assembly and supramolecular scaffolding are well suited to facilitate the implementation of multiporphyrins in solution and ultimately on surfaces. The following pages address a conceptual analysis of multi-porphyrin self-assembly through specific contributions from our research group and a comparison with selected examples from the literature.

Self-assembly via coordination

The field of self-assembly *via* coordination chemistry was initiated in the early age of multi-porphyrins by the two examples (among others) represented in Chart 5.[25,26] In the ground state of both compounds, each porphyrin macrocycle is independent. The electronic interactions between the chromophores are inefficient because of the *ca.* 60° dihedral angle between the phenyl groups and the porphyrin plane and, also due to the free rotation around the longitudinal axis of the scaffold. To attain a geometrical control of the respective orientation of each building block, secondary interactions can be added to a primary coordination bond. These additional non-covalent bonds are generally labile, yet possibly directional interactions. The latter will be used to finely tune the spatial organisation of two building blocks.[27]

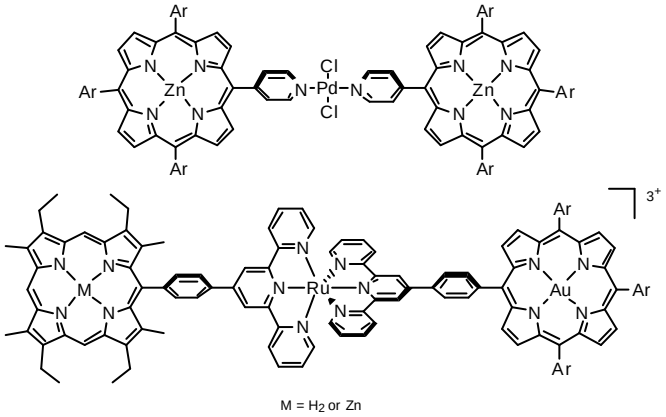

Chart 5. Two examples of porphyrin dimers linked by coordination complexes of Pd^{II} and Ru^{II}.**Erreur ! Signet non défini.Erreur ! Signet non défini.**

The frequent presence of a central metal in the porphyrin core not only allows fine-tuning of the electronic structure of the chromophores, but also offers a coordination site for an axial base.[28] The binding of an axial base corresponds to the formation of endogen coordination complexes (Chart 6), whereas the formation of peripheral coordination complexes at an external binding site corresponds to an exogen coordination. In this case, the metal core in the porphyrin does not intervene in the assembly process.

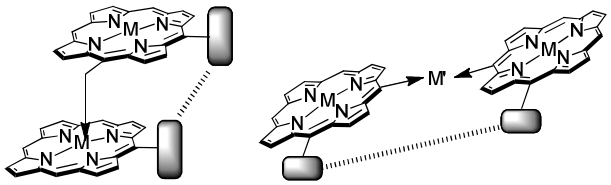

Chart 6. Limitation of the conformational freedom around coordination bonds represented by arrows, by adding a complementary weak interaction (dotted line).

Peripheral coordination: Stepwise self-assembly

One of the first examples of peripheral coordination *via* chelation was reported by Barrett and Hoffman[29] for a dithiolato-porphyrazine (Chart 7), a structural analogue of porphyrin. Strong interactions were observed between the two macrocycles.

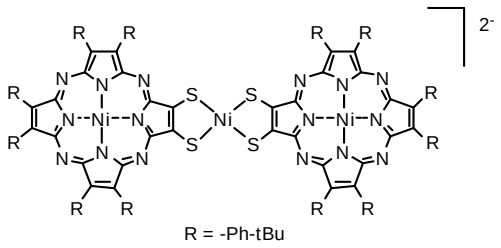

R = -Ph-tBu

Chart 7. An example of peripheral metallic coordination on porphyrazines.

Around the same period, our contribution to the field started with an initial interest in the peripheral modification of the porphyrin macrocycle. According to the synthetic pathway depicted in Scheme 2, a porphyrin in which one *meso*-aryl group was fused to the neighbouring pyrrole was obtained in four steps.[30] Taking advantage of the reactivity of the β-position next to the carbonyl group, the corresponding enamino-ketone was prepared in good overall yields using the Katritsky reagent.[31] The versatility of the synthesis provided

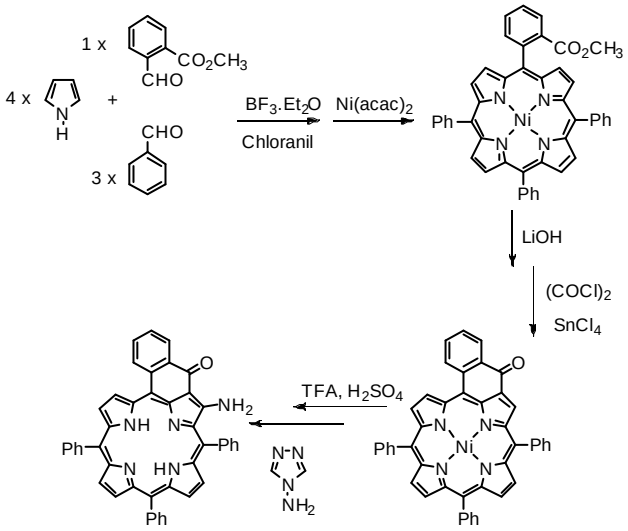

Scheme 2. Synthesis of the enaminoketone building block.

several porphyrin macrocycles with various symmetries bearing one or two exocyclic chelating sites.[32] Moreover, the reaction of the enaminoketone with Lawesson's reagent[33] led to the replacement of the oxygen atom by sulphur, thus increasing the number of combinations of metals that can be bound to the peripheral chelates. In the last decade, a wide range of multimetallic complexes has been constructed according to the general strategy depicted in Scheme 3.[34] Furthermore, the versatility of this approach and the use of adequate metal salts permitted the stepwise formation of metal-linked dimers.

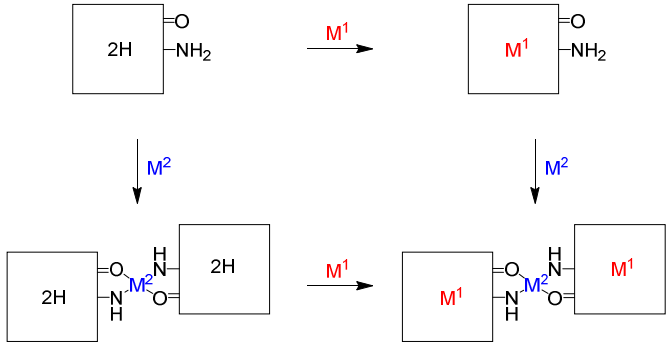

Scheme 3. Metallation of enaminoketone and stepwise combination of metals in a single architecture.

The first evidence for electronic communication in the dimers was provided by electrochemical measurements that showed two characteristic features: first, a decrease of the electrochemical gap (ΔE) between the first oxidation and the first reduction potentials of the two identical chromophores, and second, the splitting of the first oxidation potential of the porphyrin macrocycles. These features are illustrated in Figure 3 for porphyrin dimers constructed from the building block in Scheme 2.

Cyclic voltammetry (CV) clearly shows that, for example, the first oxidation signal of the Ni monomer in Figure 3a is converted into a split signal in the voltammogram of the Ni

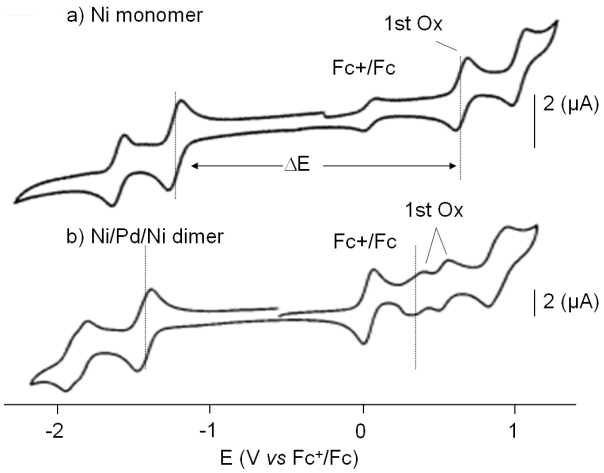

Figure 3. Electrochemical features of a nickel-porphyrin and its corresponding dimer assembled around palladium(II).

dimer linked by Pd^{II}. Similar behaviour was observed for all dimers and for the building block described in Scheme 2. Significant data are summarized in Table 1.

Small variations in the synthetic pathway of Scheme 3 have generated a wide variety of chelates and bis-chelates, such as those represented in Chart 8. These compounds differ by the nature of the heteroatom X (keto or thioketone), the aryl groups at *meso* positions and/or the the central metal. The combination of these bis-chelate and mono-chelate building blocks has afforded a variety of scaffolds, ranging from dimers to tetramers.[35]

Table 1. UV-visible and electrochemical data for porphyrin dimers and various metal complexes combinations. Standard conditions: solvent: CH_2Cl_2, containing 0.1 M $(n\text{-}Bu)_4NPF_6$ for CV experiments.

$M^1/M^2/M^1$	λ_{max} (ε)	ΔE (eV)	Observed splitting $E_{ox2} - E_{ox1}$ (eV)
Ni/Ni/Ni	700 (32 800)	1.77	0.16
Ni/Cu/Ni	677 (30 000)	1.83	0.17
Ni/Pd/Ni	696 (47 100)	1.78	0.16
Cu/Pd/Cu	696 (45 100)	1.78	0.16

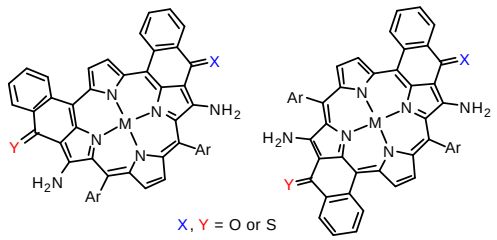

Chart 8. Versatile building blocks for porphyrin oligomers.

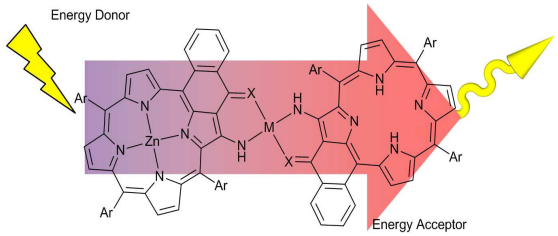

Table 2. Energy transfer times between the energy donor and acceptor after irradiation, splitting of the first oxidation waves and d orbital contribution to the overall electronic density for three photochemical dyads.

X	M	Time of transfer (fs)	Splitting $E_{ox2} - E_{ox1}$ (eV) Ni/M/Ni	d orbital contribution (%)
O	Pd	660	0,16	4.6
O	Pt	105	0,22	11.2
S	Pt	< 50	0.28	13.5

The extremely efficient delocalisation of the electronic density in these species led to very interesting properties of the resulting chromophores. In particular, the versatility of the synthetic approach led to a series of photochemical dyads comprising a zinc porphyrin and a free base porphyrin that respectively act as an energy donor and an energy acceptor upon photoexcitation. As reported in Table 2, the energy transfer was markedly faster by replacing palladium(II) by platinum(II) as the linker or by introducing sulphur instead of oxygen in the chelate unit. In addition, the splitting of the first oxidation increased to values similar to those reported for covalently linked, conjugated dimers. These variations were corroborated by DFT calculations. The participation of the d orbitals to the overall electronic density was found to increase with the extent of delocalisation.[36-39]

Coordination to the central metal

Self-assembly *via* coordination to the central metal has been widely used to generate multiporphyrin scaffolds, mostly through the use of iterative, self-coordinating motifs, that form 3D architectures.[40] However, all approaches leading to multiporphyrin architectures are confronted with the question of entropy, which drives the self-assembly towards discrete species rather than towards oligomers. In solution, multiporphyrin assembling induced by coordination to a central metal generally leads to 3D molecular boxes,[41] but can also lead to various morphologies depending on experimental conditions.[42] However, when associated with other interactions or with the adequate orientation of the binding groups, infinite arrays can be produced. In general, the morphology of these arrays is controlled in the solid state.[42,43,44] For example, to control the linear morphology of assemblies *via* coordination of the metallic porphyrin core, both dimerization[45] and the use of porphyrins bearing two peripheral metal-binding ligands at 5 and 15 *meso* positions is a simple, yet efficient design, as shown in Chart 9.[46]

In the course of our work on synthetic models of cytochrome c oxidase, a phenanthroline-strapped porphyrin

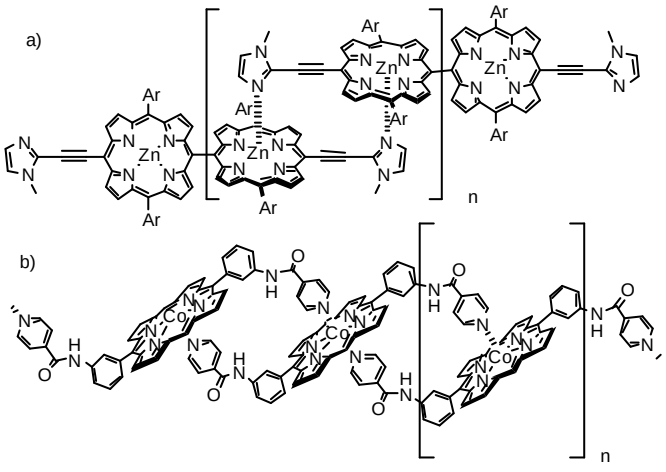

Chart 9. Linear porphyrin architectures assembled by coordination of imidazole to a central metal of the porphyrin.

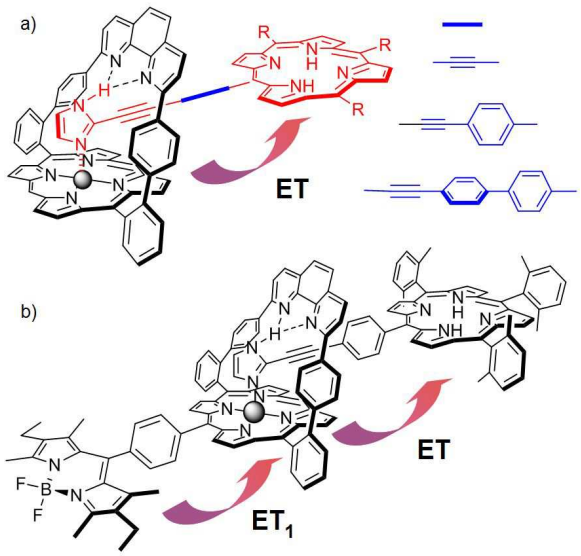

Figure 4. Dyads and triads built using the selective binding of imidazoles in a phenanthroline-strapped porphyrin.

was prepared by a highly efficient synthetic approach.[47] This particular strapped-porphyrin has shown impressive recognition behaviour towards *N*-unsubstituted imidazole derivatives with binding constants ranging from as high as 10^7 M^{-1} in the case of the 2-methylimidazole[48] to 10^5 M^{-1} for the more hindered 2-methylbenzimidazole.[49] Taking advantage of this recognition process and the well-defined orientation of the imidazole within the phenanthroline pocket, the photochemical dyads and triads depicted in Figure 4 were prepared.

The efficiency of the energy transfer (ET) in the dyads (Figure 4a) was optimized to reach 99% by varying the nature and the length of the linkers between the two subunits. Due to the absence of orbital overlap between the zinc and free base porphyrins, a pure Förster mechanism was proposed for the energy transfer.[50] To introduce an energy input (ET_1) independent of the zinc porphyrin, a boron-dipyrrin component was included in the corresponding triads.[51] A similar strategy was previously proposed in the pioneering work of Lindsey.[15]

This imidazole-based self-assembly was then employed as a soft method for the preparation of porphyrin oligomers. The first attempts using the iterative motif represented in Chart 10 rapidly faced entropy issues during the self-assembly process in solution (illustrated in blue in c and d). Indeed, these building blocks formed symmetrical homo-dimers with very high association constants (10^9 M^{-1}).[52] The inhibition of the dimer formation strongly depends on the ability of the solvent to compete with the coordination of imidazole within the phenanthroline strap. Pyridine has been the best choice to generate self-assembled linear wires reaching up to a few hundred porphyrins. The imidazole coordination occurs in a well-defined orientation and the resulting geometrical control on the formation of straight linear oligomers[53] on mica (Figure 5) compares favourably with other reported oligomers.[45]

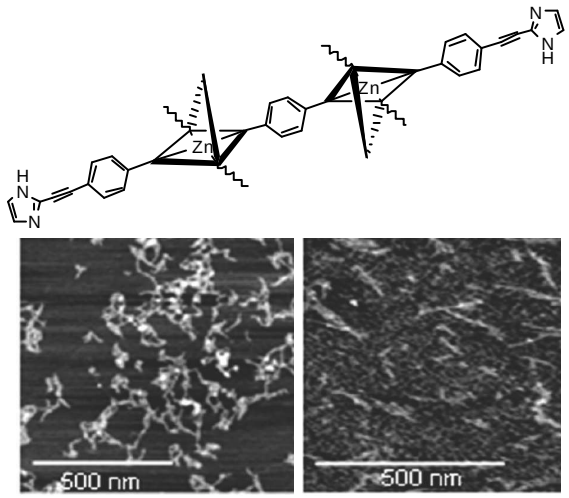

Figure 5. Formation of wires using the association of porphyrin dimers.

The final utilisation of any molecular wire requires its deposition on a given surface; therefore, a general field of research has emerged regarding the surface-assisted or surface-driven self-organisation of organic materials.[54] In metal-mediated self-assembly, *via* external or internal coordination, current work is oriented towards the use of surface deposition in the formation of self-assembled porphyrin wires. Early results are summarized in the last section of this article.

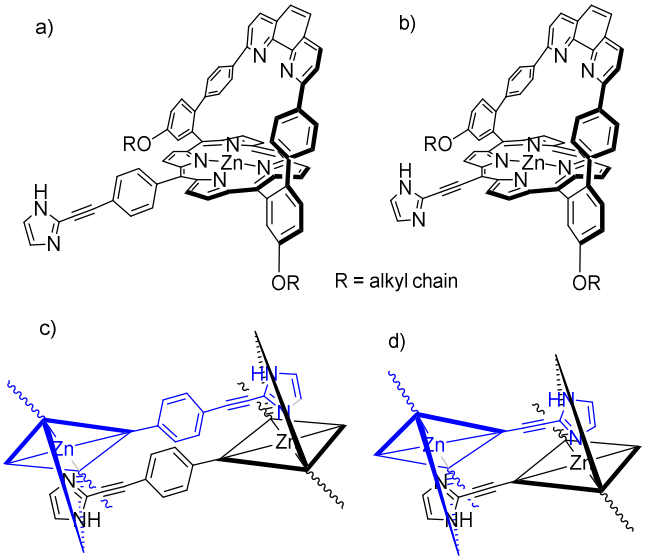

Chart 10. Iterative motifs (top) of imidazole-functionalized strapped porphyrins and their cartoon representations.

Self-assembly at the solid-liquid interface

Peripheral coordination

The use of surfaces to organise and assemble molecular materials requires the control of sets of molecule-surface interactions comprising π-stacking, hydrophobic interactions, and/or van der Waals interactions. These interactions need to

be included in the design of the self-assembly process to complement a molecular recognition event, namely the metal ion binding in the present case. The use of a liquid phase for the deposition of the building blocks on a substrate generally requires the presence of remote solubilising groups that do not interfere with the metal coordination. To illustrate this purpose, porphyrins bearing external coordination sites were modified by the addition of alkyl chains to the *meso* aryl groups, as depicted in Chart 11.

Preliminary studies show that both the building blocks and

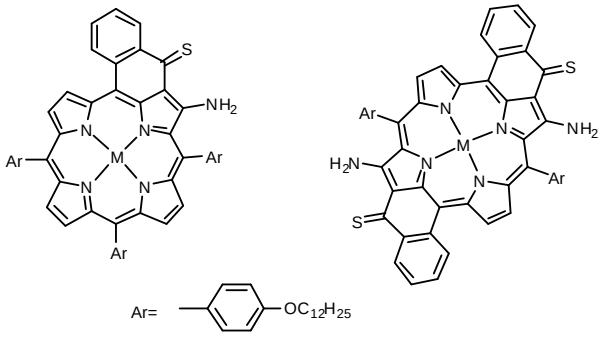

Chart 11. Examples of porphyrins bearing external coordination sites and alkoxyphenyl groups.

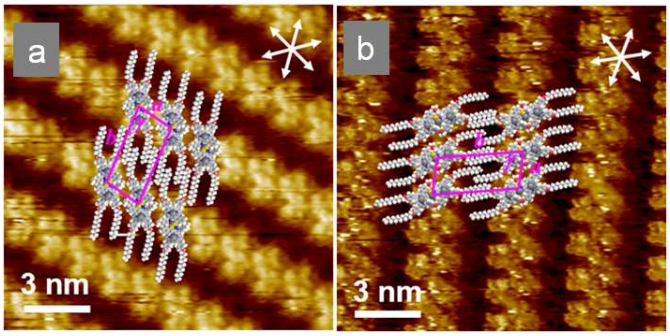

Figure 5. STM images of the organised assemblies formed on HOPG from the mono-chelate in Chart 11.

the dimers obtained after metal coordination were able to self-organise on a Highly Oriented Pyrolitic Graphite (HOPG) surface as demonstrated by the STM images collected for the mono-chelate (Figure 5a). This building block associates via H-bonding of two enamino-thioketones and adopts a similar arrangement after insertion of the central metal (Pd) (Figure 5b).[55] The next step in this field is to demonstrate that the coordination can take place on the surface using pre-adsorbed bis-chelates (Chart 11).

Central metal coordination

As discussed before for the phenanthroline-strapped porphyrin building blocks, the preferred formation of dimers in solution results from entropy-driven processes. This preference can be modified by introducing additional interactions with a surface. The presence of molecule-surface interactions, such as non-directional π-stacking of the

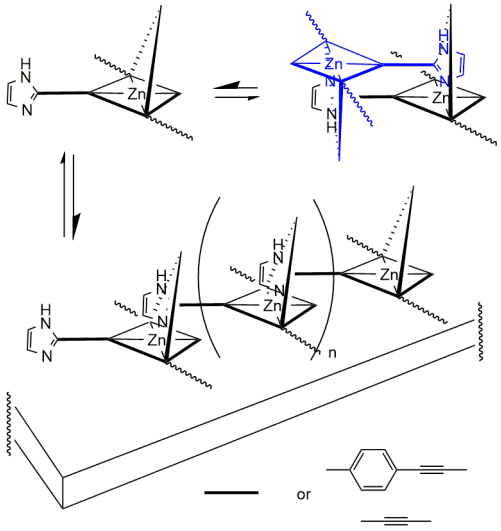

Scheme 4. The presence of monomers in solution is necessary for the surface-assisted formation of porphyrin wires on a surface.

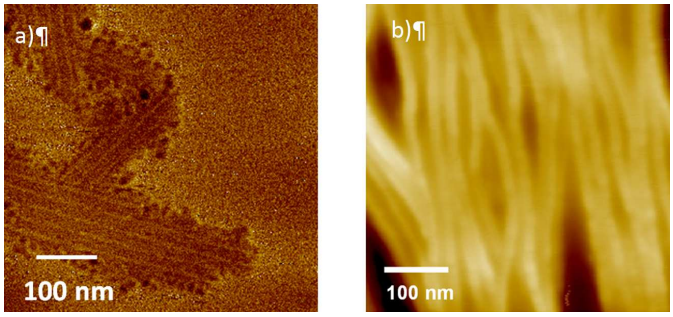

Figure 6. Examples of surface and solvent controlled morphologies of self-assemble porphyrin wires.

porphyrin with HOPG and oriented CH-π interactions of alkyl chains with the graphite plane, confines the intermolecular interactions in the 2D space. *In fine*, molecule-surface interactions and progressive quenching of monomers perturb the monomer/dimer equilibrium.[56] Adsorption on the surface competes with the formation of dimers, thus the self-assembly process takes place in a film of solvent on the surface, as depicted in Scheme 4.

The hydrophobic interaction of the flat porphyrin surface with the solid substrate (e.g. HOPG) can be roughly tuned and enhanced by increasing the polarity and the coordinating properties of the solvent. Over the years, the deposition method used for the phenanthroline-strapped derivatives has been standardised, first using pyridine to dissociate the dimers in solution into monomers, and then diluting stock solutions of the pyridine-bound monomers in a solvent used for deposition. The AFM images in Figure 6 show critical examples of how the solvent affects surface-bound objects obtained with phenanthroline-strapped building blocks.

When methylcyclohexane was used as a deposition solvent, the quenching of monomers on the surface is a slow process and the directionality imposed by the surface is strong. The AFM image (Figure 6a) shows islands of aligned, single

molecular wires oriented according to the surface symmetry. With time, this first organised layer can serve as a template for growth of the objects along the "z" direction (orthogonal to the surface; not shown).[57]

In methylene chloride, the porphyrin macrocycle is extremely soluble and the side chains interact less with the solvent and more with each other. As a result, side-by-side aggregation led to the formation of bundles of fibres comprising several self-assembled porphyrin wires (Figure 6b). In order to interface the self-assembled wires with dielectric surfaces,[58] a similar approach was developed with polyoxy-ethylene side chains; rather long self-assembled porphyrin wires were observed on mica after 24 hours of incubation with the surface after deposition.[57] At this stage, the interfacing of porphyrin wires with carbon nanotubes is in progress, especially to construct porphyrin brushes that can be used as photonic energy collectors.

Conclusions

The design of self-assembled materials at the nanoscale requires the precise programming of sets of interactions. These interactions range from the driving force of strong primary interactions to weaker or secondary interactions which finely tune the morphology of the assemblies. In the case of porphyrins, the strong primary interaction can consist of metal binding, either in the porphyrin core or at its periphery. Controlling the morphology of the edifice is a prerequisite to the investigation and understanding of the electronic properties of the self-assembled materials. Finally, the necessary interfacing of self-assembled materials with surfaces in prospective applications strongly suggests that molecule-surface interactions should be included in the toolbox of supramolecular functional self-assembly.

Acknowledgements

This work has benefited from a constant support of the CNRS, the University of Strasbourg, the Japan Society for the Promotion of Science (JSPS), The Agence Nationale de la Recherche (ANR) and the Japanese Science and Technology (JST) agency. It has also benefited from periodical support from the French Ministry of Research who provided financial support to PhD students whose names appear in the references and who have been involved in sometime difficult synthesis and tedious purifications without losing their hope or their smile.

Notes and references

1. A. R. Battersby, *Nat. Prod. Rep.*, 2000, **17**, 507.
2. J. Deisenhofer, O. Epp, K. Miki, R. Huber and H. Michel, *Nature*, 1985, **318**, 618; Figure 1 was produced using the PDB file 1prc released in J. Deisenhofer, O. Epp, I. Sinning and H. Michel, *J. Mol. Biol.*, 1995, **246**, 429.
3. a) J. L. Sessler, J. Hugdahl and M. R. Johnson, *J. Org. Chem.*, 1986, **51**, 2838; b) A similar approach was developed with a naphthalene spacer: A. Osuka and K. Maruyama *J. Am. Chem. Soc.*, 1988, **110**, 4454.
4. S. Noblat, C. O. Dietrich-Buchecker and J.-P. Sauvage, *Tetrahedron Lett.*, 1987, **28**, 5829.
5. W. Kühlbrandt, D. N. Wang and Y. Fujiyoshi, *Nature*, 1994, **367**, 614.
6. G. McDermott, S. M. Prince, A. A. Freer, A. M. Hawthornthwaite-Lawless, M. Z. Papiz, R. J. Cogdell and N. W. Isaacs, *Nature*, 1995, **374**, 517.
7. R. J. Cogdell, N. W Isaacs, A. A. Freer, T. D. Howard, A. T. Gardiner, S. M. Prince and M. Z. Papiz, *FEBS Lett.*, 2003, **555**, 35.
8. M. Z. Papiz, S. M. Prince, T. Howard, R. J. Cogdell and N. W. Isaacs, *J.Mol.Biol.*, 2003, **326**, 1523.
9. D. L. Dexter, *J. Chem. Phys.*, 1953, **21**, 836.
10. T. Förster, *Ann. Phys.*, 1948, **2**, 55.
11. J. M. Ribò, J. M. Bofill, J. Crusats and R. Rubires, *Chem. Eur. J.*, 2001, **7**, 2733.
12. S. Scheuring, J. Seguin, S. Marco, D. Lévy, B. Robert and J.-L. Rigaud, *Proc. Nat. Acad. Sci*., 2003, **100**, 1690 and references cited therein.
13. J.-S. Hsiao, B. P. Krueger, R. W. Wagner, T. E. Johnson, J. K. Delaney, D. C. Mauzerall, G. R. Fleming, J. S. Lindsey, D. F. Bocian and R. J. Donohoe, *J. Am. Chem. Soc*., 1996, **118**, 11181.
14. a) The idea of a "molecular rectifier" was originally coined in a theoretical paper by A. Aviram and M. A. Ratner, *Chem. Phys. Lett*., 1974, **29**, 277; b) For a revisited and deeper analysis please see A. Nitzan and M. A. Ratner, *Science*, 2003, **300**, 1384.
15. R. W. Wagner and J. S. Lindsey, *J. Am. Chem. Soc*., 1994, **116**, 9759.
16. J. S. Lindsey, S. Prathapan, T. E. Johnson and R. W. Wagner, *Tetrahedron*, 1994, **50**, 8941.
17. V. S.-Y. Lin, S. G. DiMagno and M. J. Therien, *Science*, 1994, **264**, 1105.
18. A. Osuka and H. Shimidzu, *Angew. Chem. Int. Ed. Engl.*, 1997, **36**, 135.
19. A. Tsuda, A. Nakano, H. Furuta, H. Yamochi and A. Osuka, *Angew. Chem. Int. Ed. Engl.*, 2000, **39**, 558.
20. D. H. Yoon, S. B. Lee, K.-H. Yoo, J. Kim, J. K. Lim, N. Aratani, A. Tsuda, A. Osuka and D. Kim, *J. Am. Chem. Soc.*, 2003, **125**, 11062.
21. a) M. Gilbert and B. Albinsson, *Chem. Soc. Rev.*, 2015, **44**, 845; b) T. Tanaka and A. Osuka, *Chem. Soc. Rev.*, 2015, **44**, 943.
22. F. Fages, J. A. Wytko and J. Weiss, *C. R. Chimie*, 2008, **11**, 1241.
23. J. A. Wytko and J. Weiss, in *N4-Macrocyclic metal complexes: Electrocatalysis, electrophotochemistry & biomimetic electroanalysis*, ed. J. Zagal, F. Bedioui, J. P. Dodelet, Springer, New York, 2006, Chapter 13, 603-724.
24. N. Aratani, A. Takagi, Y. Yanagawa, T. Matsumoto, T. Kawai, Z. S. Yoon, D. Kim and A. Osuka, *Chem. Eur. J*., 2005, **11**, 3389.
25. C. M. Drain and J.-M. Lehn, *J. Chem. Soc., Chem. Commun*., 1994, 2313.
26. A. Harriman, F. Odobel and J.-P. Sauvage, *J. Am. Chem. Soc*., 1994, **116**, 5481.
27. J. Weiss, M. Koepf and J. A. Wytko, in *Supramolecular Chemistry: from Molecules to Nanomaterials*, eds. J. W.

Steed and P. A. Gale, John Wiley & Sons Ltd, Chichester, UK, 2012, 2115-2147.
28. J. Weiss, *J. Inclusion Phenom. Macrocyclic Chem*., 2001, **40**, 1 and references cited therein.
29. T. F. Baumann, A. G. M. Barrett and B. M. Hoffman, *Inorg. Chem*., 1997, **36**, 5661.
30. S. Richeter, C. Jeandon, C. Sauber, J.-P. Gisselbrecht, R. Ruppert and H. J. Callot, *J. Porphyrins Phthalocyanines*, 2002, **6**, 423.
31. A. R. Katritzky and K. S. Laurenzo, *J. Org. Chem*., 1988, **53**, 3978.
32. S. Richeter, C. Jeandon, N. Kyritsakas, R. Ruppert and H. J. Callot, *J. Org. Chem.*, 2003, **68**, 9200.
33. I. Thomsen, K. Clausen, S. Scheibye, and S.-O. Lawesson, *Org. Synth. Coll.*, 1990, **7**, 372.
34. S. Richeter, C. Jeandon, R. Ruppert and H. J. Callot, *Chem. Commun*., 2002, 266.
35. H. J. Callot, R. Ruppert, C. Jeandon and S. Richeter, *J. Porphyrins Phthalocyanines*, 2004, **8**, 111.
36. H. Dekkiche, A. Buisson, A. Langlois, P.-L. Karsenti, L. Ruhlmann, R. Ruppert and P. D. Harvey, *Chem. Eur. J.*, 2016, **22**, 10484.
37. H. Dekkiche, A. Buisson, A. Langlois, P.-L. Karsenti, L. Ruhlmann, P. D. Harvey and R. Ruppert, *Inorg. Chem.*, 2016, **55**, 10329.
38. M. Abdelhameed, P.-L. Karsenti, A. Langlois, J.-F. Lefebvre, S. Richeter, R. Ruppert and P. D. Harvey, *Chem. Eur. J.*, 2014, **20**, 12988.
39. M. Abdelhameed, A. Langlois, P.-L. Karsenti, S. Richeter, R. Ruppert and P. D. Harvey, *Chem. Commun*., 2014, **50**, 14609.
40. G. Ercolani, M. Ioele and D. Monti, *New J. Chem.*, 2001, **25**, 783.
41. E. Iengo, E. Zangrando and E. Alessio, *Acc. Chem. Res.*, 2006, **39**, 841.
42. C. Oliveras-González, F. Di Meo, A. González-Campo, D. Beljonne, P. Norman, M. Simón-Sorbed, M. Linares and D. B. Amabilino, *J. Am. Chem. Soc.*, 2015, **137**, 15795.
43. E. Stulz, S. M. Scott, Y.-F. Ng, A. D. Bond, S. J. Teat, S. L. Darling, N. Feeder and J. K. M. Sanders, *Inorg. Chem*., 2003, **42**, 6564.
44. H. Lee, Y.-H. Jeong, J.-H. Kim, I. Kim, E. Lee and W.-D. Jang, *J. Am. Chem. Soc*., 2015, **137**, 12394.
45. K. Ogawa and Y. Kobuke, *J. Photochem. Photobiol. C: Photochem. Rev*., 2006, **7**, 1 and references cited therein.
46. R. A. Haycock, C. A. Hunter, D. A. James, U. Michelsen and L. R. Sutton, *Org. Lett*., 2000, **2**, 2435.
47. J. A. Wytko, E. Graf and J. Weiss, *J. Org. Chem*., 1992, **57**, 1015.
48. J. Froidevaux, P. Ochsenbein, M. Bonin, K. Schenk, P. Maltese, J.-P. Gisselbrecht and J. Weiss, *J. Am. Chem. Soc*., 1997, **119**, 12362.
49. a) D. Paul, F. Melin, C. Hirtz, J. Wytko, P. Ochsenbein, M. Bonin, K. Schenk, P. Maltese and J. Weiss, *Inorg. Chem*., 2003, **42**, 3779; b) J. Brandel, A. Trabolsi, F. Melin, M. Elhabiri, J. Weiss and A.-M. Albrecht-Gary, *Inorg. Chem*., 2007, **46**, 9534; c) J. Brandel, A. Trabolsi, H. Traboulsi, F. Melin, M. Koepf, J. A. Wytko, M. Elhabiri, J. Weiss and A.-M. Albrecht-Gary, *Inorg.Chem*., 2009, **48**, 3743.
50. a) D. Paul, J. Wytko, M. Koepf and J. Weiss, *Inorg. Chem*., 2002, **41**, 3699 ; b) I. Leray, B. Valeur, D. Paul, E. Regnier, M. Koepf, J. A. Wytko, C. Boudon and J. Weiss, *Photochem. Photobiol. Sci*., 2005, **4**, 280.
51. M. Koepf, A. Trabolsi, M. Elhabiri, J. A. Wytko, D. Paul, A. M. Albrecht-Gary and J. Weiss, *Org. Lett*., 2005, **7**, 1279.
52. M. Koepf, J. A. Wytko, J.-P. Bucher and J. Weiss, J. *Am. Chem. Soc*., 2008, **130**, 9994.
53. M. Koepf, J. Conradt, J. Szmytkowski, J. A. Wytko, L. Allouche, H. Kalt, T. S. Balaban and J. Weiss, *Inorg. Chem*., 2011, **50**, 6073.
54. M. Koepf, F. Cherioux, J. A. Wytko and J. Weiss, *Coord. Chem. Rev.*, 2012, **256**, 2872.
55. M.-A. Carvalho, H. Dekkiche, L. Karmazin, F. Sanchez, B. Vincent, M. Kanesato, Y. Kikkawa and R. Ruppert, *Inorg. Chem.*, *in press*, DOI: 10.1021/acs.inorgchem.7b02422.
56. V. Rauch, J. A. Wytko, M. Takahashi, Y. Kikkawa, M. Kanesato and J. Weiss, *Org. Lett.*, 2012, **14**, 1998.
57. V. Rauch, Y. Kikkawa, M. Koepf, I. Hijazi, J. A. Wytko, S. Campidelli, A. Goujon, M. Kanesato and J. Weiss, *Chem. Eur. J.*, 2015, **21**, 13437.
58. V. Rauch, J. Conradt, M. Takahashi, M. Kanesato, J. A. Wytko, Y. Kikkawa, H. Kalt and J. Weiss, *J. Porphyrins Phthalocyanines*, 2014, **18**, 67.